

Evidence from Earthquake Data for a Partially Molten Crustal Layer in Southern Tibet

Rainer Kind, James Ni,* Wenjin Zhao, Jianxin Wu, Xiaohui Yuan, Lianshe Zhao, Eric Sandvol, Chris Reese, John Nabelek, Thomas Hearn

Earthquake data collected by the INDEPTH-II Passive-Source Experiment show that there is a substantial south to north variation in the velocity structure of the crust beneath southern Tibet. North of the Zangbo suture, beneath the southern Lhasa block, a mid-crustal low-velocity zone is revealed by inversion of receiver functions, Rayleigh-wave phase velocities, and modeling of the radial component of teleseismic *P*-waveforms. Conversely, to the south beneath the Tethyan Himalaya, no low-velocity zone was observed. The presence of the midcrustal low-velocity zone in the north implies that a partially molten layer is in the middle crust beneath the northern Yadong-Gulu rift and possibly much of southern Tibet.

The 1994 INDEPTH-II Passive-Source Experiment yielded high-quality earthquake data with which to analyze the interaction between the Indian and Eurasian plates. A 15-station passive recording array was deployed, extending from the High Himalaya to approximately 150 km north of the Zangbo suture [figure 1 of (1)]. Nine of the stations were equipped with broad-band Guralp CMG-3T seismometers with a usable frequency range of 0.01 to 30 Hz; the remaining six stations were equipped with Mark Products 1-Hz L-4 seismometers. Each station had one data stream that continuously recorded 24-bit data at 50 samples per second. From May to October 1994, approximately 200 earthquakes were recorded. Using these data we examined the velocity structure of the crust beneath the INDEPTH-II survey by receiver-function analysis, surface wave dispersion, and *P*-waveform modeling.

Receiver-function analysis was undertaken using seismograms from approximately 17 earthquakes recorded at each station (2). Most of the earthquakes that were used occurred in two regions: the northwest Pacific and Indonesia. Processed seismograms were stacked to enhance the *P*-to-*S* converted phases. The station spacing in the array was up to a few tens of kilometers and thus too large to expect phases that can be

correlated from one station to the next. In order to improve the coherence between stations we used a moving average technique that sums the individual receiver function from three adjacent stations. In effect, this procedure corresponds to a spatial long-period filter and de-emphasizes short-period variations from station to station. All of the summed receiver functions for averaged stations north of the suture contain strong energy between 0 and 10 s and a prominent, negative amplitude phase that arrived about 2 s after the direct *P* phase.

We used the iterative inversion method

of Kind *et al.* (3) to produce one-dimensional shear-wave velocity models for the averaged receiver function. The independent parameter in the inversion was the shear-wave velocity (V_s) which was related to the *P*-wave velocity through a fixed V_p/V_s ratio of 1.73. Synthetic *Q* components (2) were computed using the Thompson-Haskell matrix method (4) for an average angle of incidence (averaged over all epicentral distances between events and stations). We rotated the theoretical traces and deconvolved them like the observed traces and found the optimal parameters for each model by iteratively minimizing the mean square deviation of the observed and model-generated traces. Figure 1 shows the initial and final velocity models and corresponding waveforms for the averaged receiver functions A36 and A18 observed north and south of the suture, respectively (5). The most striking feature in the final velocity model is the low-velocity zone in the middle crust north of the suture, beginning at a depth of about 20 km. This feature is obtained for all averaged stations located north of the suture. Inversion of seismogram A36 requires that the Moho is at a depth of about 80 km to fit a phase at about 9.6 s (Fig. 1). All stations to the south of Lhasa have this phase, which is likely the conversion at the Moho. Inversion results for stations located south of the suture do not show a mid-crustal low-velocity zone (bottom of Fig. 1). Crustal models from these southern stations show that the upper crust

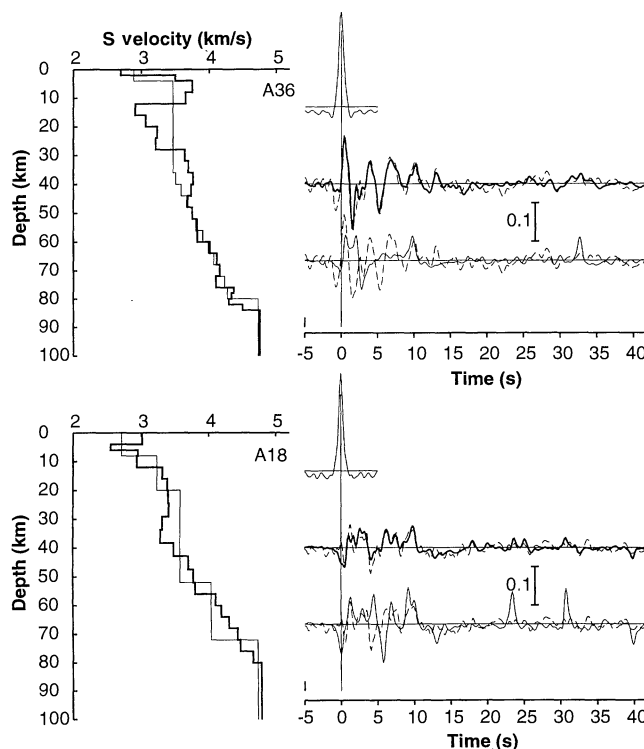


Fig. 1. Inversion of the averaged receiver function A36 and A18. Starting and final models are the thin and heavy lines in the left half of the figure, respectively. For each subplot, the dashed lines in the right half of the figure are the observed receiver functions. The thin line in the bottom traces is the theoretical receiver function belonging to the starting model. The heavy line in the middle traces on the right belongs to the final model and matches the data well. The top trace on the right of each subplot is the input *P* signal, which has normalized amplitude.

R. Kind and Xiaohui Yuan, GeoForschungsZentrum Potsdam, 14473 Potsdam, Germany.
James Ni, Jianxin Wu, C. Reese, T. Hearn, Department of Physics, New Mexico State University, Las Cruces, NM 88003, USA.
Wenjin Zhao, Chinese Academy of Geological Sciences, Beijing, China
Lianshe Zhao, Institute for Geophysics, University of Texas at Austin, Austin, TX 78759, USA.
E. Sandvol, Department of Geological Sciences, Cornell University, Ithaca, NY 14853, USA.
J. Nabelek, College of Oceanography, Oregon State University, Corvallis, OR 97331, USA.

*To whom correspondence should be addressed.

is approximately 40 km thick and has a low average crustal shear-wave velocity of about 3.4 to 3.5 km/s overlying a lower crust with a strong gradient. Comparison with the INDEPTH-I CMP section [figure 1 of (6)] suggests that the upper crustal layer corresponds to the upper plate that lies above the Main Himalayan thrust fault, and the lower layer corresponds to the underthrusting Indian crust. Additionally, results show that the Moho is at constant depth between stations SP25 and SP12 beneath the suture, suggesting that the suture does not penetrate the entire lithosphere.

We analyzed surface wave dispersion data for a pair of stations north of the Zangbo suture. Rayleigh wave phase-velocity dispersion data for a pure path north of the ITS were obtained from seismograms recorded at station pair BB05-BB14 from the 1 September 1994 northern California earthquake (magnitude $M_s = 7.0$). Two-station techniques were used to isolate the phase velocities of fundamental mode Rayleigh waves with periods of 20 to 60 s (Fig. 2). The California earthquake, which originated from 103° away and traveled along a mostly continental path, is well dispersed. We infer that lateral variations in Tibet do not significantly affect the phase-velocity calculations because the observed particle motion of Rayleigh waves from the California earthquake has a back azimuth similar to that computed from the stations and earthquake location (7).

Once the fundamental mode waveforms at each station were obtained (8), we inverted for an initial Earth model using interstation group velocities. A time-domain cross-correlation technique was used to refine the phase velocities. We then inverted for a new Earth model from the refined phase velocities. After four to five iterations the phase velocities could no longer be improved. We also tried to obtain the

fundamental-mode Love waves but were unsuccessful because of contamination by core phases. The error in the phase velocity is mainly contained in the computed interstation phase spectra and can be estimated by the same method used for calculating phase error of a frequency response function. In our study, the maximum and minimum phase velocity errors were ~ 0.1 and ~ 0.01 km/s, respectively.

By minimizing the error between the observed and calculated phase velocities with an iterative least square method, we obtained a best fitting model for the crust between BB05 and BB14 (Fig. 2). This model shows a 70-km-thick crust overlying an upper mantle with a fast S-wave velocity of about 4.8 km/s. The crust is characterized by a low average S-wave velocity of about 3.45 km/s (~ 6.0 km/s in P wave), a 20-km thick mid-crustal low-velocity zone of 3.0 to 3.1 km/s, and a high-velocity lower crust.

P-waveform modeling was undertaken using the second-order radial vertical comparison method (SORVEC) of Zhao and Frohlich (9) in which a radial-component seismogram is calculated from vertical-component observations. This can then be compared iteratively with a large number of model-generated synthetic radial-component seismograms using a very fast simulated annealing method (9).

The INDEPTH-II array produced teleseismic recordings of sufficient quality from 14 earthquakes with back azimuths between 45° to 157° and one with a back azimuth of 247°. The back azimuth coverage is not ideal. For each earthquake-station pair, the inversion was carried out on the recorded body waves and optimum four-layer and five-layer velocity models (layer thickness is not fixed in each inversion) were obtained. All the available vertical- and radial-component waveform data for each station were merged into a single in-

version, and an average model for each station was calculated (Fig. 3). The models for the stations north of the suture exhibit a distinct low-velocity zone below a depth of about 20 km. In general, the upper crust velocity is well constrained by the data with an uncertainty of about ± 0.15 km/s for S-wave velocity. The uncertainty is somewhat larger at greater depths. The depth of the Moho is not tightly constrained but lies between 70 and 80 km. South of the suture, beneath the Tethyan Himalaya, the model yields an average crustal thickness of about 70 km and shows no mid-crustal low-velocity zone. The velocity increases gradually with depth in the upper crust and more rapidly in the deep crust, and the lower crustal velocity gradient is similar to that observed to the north (Fig. 3).

In summary, receiver function analysis, two-station Rayleigh wave-phase velocity dispersion, and P-waveform modeling of the INDEPTH-II broadband data give consistent, independent views of the velocity structure of the crust beneath the INDEPTH-II survey. North of the Zangbo suture there is a distinct low-velocity zone in the crust, which dies out southward approximately at the suture. The crust beneath and north of the suture has a low average shear-wave velocity of about 3.45 km/s. The Moho, while not tightly constrained in these analyses, lies between 70 and 80 km depth along the length of the survey. As seismic velocity characteristically increases downward in crystalline continental crust, we infer that the low-velocity zone north of the suture marks a partial melt zone developed within the middle crust of the Lhasa block. The prominent bright spots imaged on the INDEPTH-II CMP profiles (6) coincide within resolution with the top of the mid-crustal low-velocity zone delineated by the earthquake data, supporting their infer-

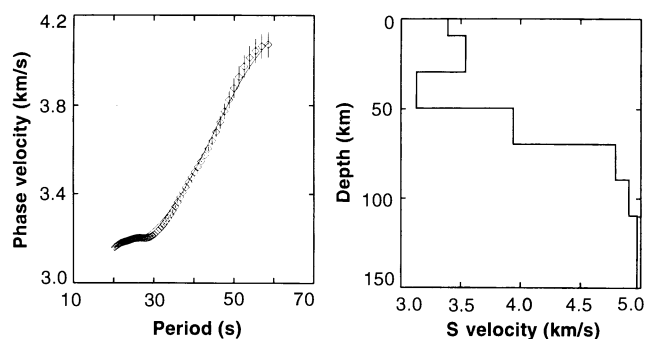
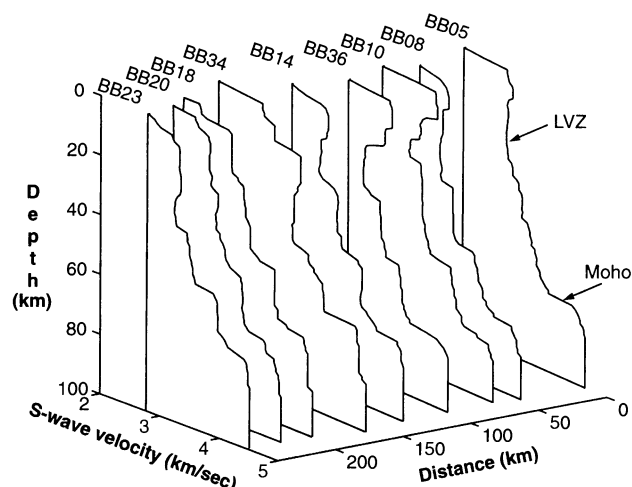


Fig. 2 (left). The fit between the observed and calculated phase velocities for the southern Tibetan Plateau are shown on the left. The vertical bars in the phase velocity plot represent errors. The best-fit model from the least squares inversion is shown on the right. **Fig. 3 (right).** Cross-section summarizing main features of the crustal shear-wave velocity along the profile from P-waveform modeling.



ence that this feature may represent an evolving intrusive boundary at the top of a partial-melt zone.

REFERENCES AND NOTES

1. K. D. Nelson *et al.*, *Science* **274**, 1684 (1996).
2. Before processing the data the ground displacement was restored at all broadband and short period stations. Each seismogram was rotated from the standard vertical, north and east coordinate system into a ray system [Longitudinal (*L*) and *T* components] using the eigenvalues of the covariance matrix for the computation of the rotation angles at a time window following the *P*-wave arrival. The *L* and *Q* components result from a rotation of *Z* (vertical) and *R* (radial) around the angle of incidence of the *P* wave. The *Q* component is perpendicular to the incoming *P* phase in the plane of incidence and contains mostly *SV* energy and little *P*-wave energy. Source equalization was accomplished by deconvolution of the *Q* component with the *P* wave of the *L* component.
3. R. Kind, G. L. Kosarev, N. V. Peterson, *Geophys. J. Int.* **121**, 191 (1995).
4. N. A. Haskell, *J. Geophys. Res.* **67**, 4751 (1990).
5. Trace A36 results from averaging receiver functions from BB10, BB36, and SP12 and trace A18 is an averaging of receiver functions from stations BB34, BB18, and BB20.
6. L. D. Brown *et al.*, *Science* **274**, 1688 (1996).
7. The two-station phase velocity dispersion of the fundamental mode Rayleigh wave was computed using programs developed by R. Herrmann. In the data analysis we first extracted the group velocity dispersion curve of the fundamental mode by applying a Gabor Transform to the recorded Rayleigh wave train. The fundamental mode Rayleigh waveforms were isolated from the recorded Rayleigh waves by applying a phase match filter.
8. J. Wu *et al.*, *Eos* **76**, F392 (1995).
9. L.-S. Zhao and C. Frohlich, *Geophys. J. Int.* **124**, 525 (1996); L.-S. Zhao, M. K. Sen, P. Stoffa, C. Frohlich, *ibid.* **125**, 355 (1996).
10. We thank I. Billings, M. Brunner, A. Fabritius, S. Klemperer, Y. Makovsky, K. Wu, and Chinese scientists in helping to collect the seismic data used in this study. This research was funded by the National Science Foundation Grant NSF EAR-9316814.

2 August 1996; accepted 5 November 1996

Electrically Conductive Crust in Southern Tibet from INDEPTH Magnetotelluric Surveying

Leshou Chen, John R. Booker, Alan G. Jones,* Nong Wu, Martyn J. Unsworth, Wenbo Wei, Handong Tan

The crust north of the Himalaya is generally electrically conductive below depths of 10 to 20 km. This conductive zone approaches the surface beneath the Kangmar dome (dipping north) and extends beneath the Zangbo suture. A profile crossing the northern Yadong-Gulu rift shows that the high conductivity region extends outside the rift, and its top within the rift coincides with a bright spot horizon imaged on the INDEPTH CMP (common midpoint) profiles. The high conductivity of the middle crust is atypical of stable continental regions and suggests that there is a regionally interconnected fluid phase in the crust of the region.

The INDEPTH magnetotelluric (MT) investigation undertaken during April to July of 1995 was designed to study the electrical structure of the lithosphere beneath southern Tibet. Two earlier MT studies were carried out in the region: A Sino-French group collected MT data in southern Tibet in the early 1980s (1), and, subsequently, MT data were collected by Chinese investigators as part of the Golmud to Yadong Global Geoscience Transect activities (2). The INDEPTH MT study provided closely spaced sites and a wide frequency bandwidth compared to these surveys, and substantiated several of their conclusions.

We acquired MT data along two lines—a main north-south line that extended from the crest of the Himalaya to near Yangbajain in the Lhasa block [100-line, figure 1 of (3)], and a northwest-southeast trending line that obliquely crossed the northern Yadong-Gulu rift near Damxung (200-line) (4). The MT data were recorded with the use of two sys-

tems: a five-component commercial wide-band system (Phoenix V5) for shallow probing, and 20 five-component recording systems (GSC LIMS) for deeper penetration (5, 6). During the period of LIMS acquisition, 24 March to 31 July 1995, sunspot activity was low, resulting in poor signal. We compensated for this by recording for a longer interval at each location than originally planned (4 to 5 weeks instead of 2 to 3 weeks), resulting in fewer total sites than planned for the experiment.

Distortion analysis (7) was applied to the MT response estimates, both in single-frequency, single-site and in multi-frequency, multi-site modes, to determine the dimensionality of the data and derive the dominant electric strike direction. The distortion models fit the data well, which implies that a two-dimensional (2D) description of regional structures is a reasonable assumption. The electric strike directions at frequencies sampling the thick Tibetan crust beneath the 100-line are frequency-independent and east-west for most sites—parallel to the regional surface geologic strike. This observation suggests that the surface geologic strike in the region is representative of structure throughout the thickness of the crust sensed by the MT survey, which is not always the case in orogenic belts (8).

For both lines, the phase difference between the electric and magnetic fields, in both polarizations of induction (9), was greater than 45° at all but a few sites and increased with increasing period. This result indicates that conductivity increases in the crust (resistivity decreases) with increasing depth (10). Apparent resistivities were low, <10 Ω · m, at frequencies less than 0.1 Hz, and for some sites the apparent resistivities were below 1 Ω · m for frequencies less than 0.01 Hz. Such pervasively low values are atypical in the continents; shield regions have apparent resistivities that are more than two orders of magnitude higher.

We modeled the MT data using 2D inversion algorithms that simultaneously searched for the smoothest as well as best-fitting models (11) (Figs. 1 and 2). The data can be fit by more complex models, but models with less structure result in unacceptable misfits.

The model for the 100-line is based on the MT and vertical-field transfer-function data at 13 frequencies, from 80 to 0.0015 Hz, from all sites, and fits the data with an average RMS misfit of 10° in phase, 5% in apparent resistivity, and 0.10 in GDS transfer function. These misfits are high, but most misfit is concentrated on data from the southernmost four sites, which were found impossible to model because their responses were inconsistent between the two modes.

The model exhibits the following first-order features that are apparent in the data, appeared in all inversions for different frequency and site subsets and different assumptions about static shifts (12), and were not influenced by the abherent responses just mentioned: (i) From approximately 150 km south of the Zangbo suture to the north end of the line, the crust is generally electrically conductive below depths of 10 to 20 km (<200 Ω · m). (ii) North of Kangmar the crust becomes extremely conductive at depth (generally much less than 30 Ω · m; “3” in Fig. 1). (iii) A north-dipping zone of high conductivity extends upward to the

Leshou Chen, Wenbo Wei, Handong Tan, China University of Geosciences, Beijing, China.

J. R. Booker, Nong Wu, M. J. Unsworth, School of Geophysics, University of Washington, Seattle, WA 98195, USA.

A. G. Jones, Geological Survey of Canada, 1 Observatory Crescent, Ottawa, Ontario, Canada K1A 0Y3.

* To whom correspondence should be addressed.